RSC Advances

ROYAL SOCIETY OF CHEMISTRY

www.rsc.org/advances

Graphic Abstract

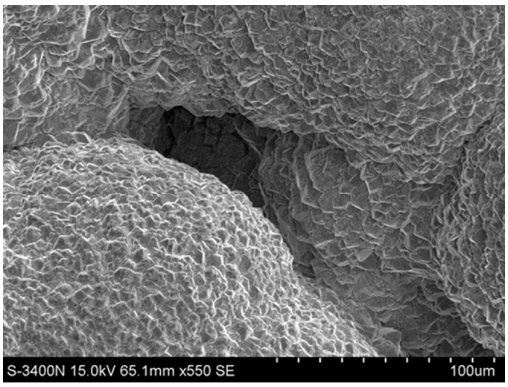

A systematic study was carried out to investigate the preparation and characterization of porous Ti/SnO_2-Sb_2O_3/PbO_2 . Porous titanium substrates contribute to the performance improvement of electrodes.

RSC Advances

RSCPublishing

ARTICLE

Study on the performance of an improved Ti/SnO_2-Sb_2O_3/PbO_2 based on porous titanium substrate compared with planar titanium substrate†

Cite this: DOI: 10.1039/xoxxoooooox

Wei Zhao, [ab] Juntao Xing,[b] Donghui Chen*[ab] Zilong Bai,[b] and Yisheng Xia,[b]

This present work focused on systematic studying the effect of porous Ti substrate on the surface structure and electrochemical properties of lead dioxide electrodes prepared by anodic deposition under galvanostaic conditions. Characterization experiments including scanning electron microscopy (SEM), X-ray diffraction (XRD), linear sweep voltammograms (LSV), cyclic voltammertry (CV), electrochemical impedance spectroscopy (EIS), accelerated life time test and degradation experiment of methylene blue trihydrate were performed to determine the effect of the different Ti substrate. Compared with planar Ti substrate, the results show that the porous Ti substrate decreased the grain size of lead dioxide and formed a compact and fine surface coating. The electrode had smaller crystal particles and more compact structure. The porous Ti/SnO_2-Sb_2O_3/PbO_2 had higher oxygen evolution overpotential, higher active surface area and higher electrochemical activity. Besides, the life of porous Ti/SnO_2-Sb_2O_3/PbO_2 (214 h) was 3.69 times as much as that of planar Ti/SnO_2-Sb_2O_3/PbO_2 electrode (58 h). Moreover, the degradation rate constant of methylene blue trihydrate on the porous Ti substrate lead dioxide (0.03868 min^{-1}) was 1.52 times that on planar Ti substrate lead dioxide (0.02542 min^{-1}).

Received ooth January 2014,
Accepted ooth January 2014

DOI: 10.1039/xoxxoooooox

www.rsc.org/

1 Introduction

In recent years, electrochemical oxidation technology as an advanced oxidation treatment for organic pollutant wastewater has attracted increasing attention due to its high energy efficiency, environmental compatibility, and easy applicability to automation[1-5]. The research hotspot of the literatures mainly focuses on the study of excellent electrode materials[6], electrochemical degradation mechanism[7], the synergistic effect of electrochemical oxidation technology and other degradation technology[8]. However, the development of electrodes with high electrochemical activity and stability is one of the key factors affecting the efficiency of electrochemical oxidation[9]. The lack of suitable anodes is still a major problem.

So far, various types of electrodes including carbon materials (such as activated carbon fiber, graphite electrode, boron doped diamond (BDD)), metal materials (such as platinum electrode, titanium metal, stainless steel) and dimensionally stable electrode (DSA) (such as, RuO_2, SnO_2 and PbO_2) have been investigated for electro-catalytic oxidation of organic pollutant[4, 5, 10, 11]. Comparison of various electrodes has shown that metal oxide electrode based on titanium substrate and BDD electrode is one of the most suitable electrodes for electrochemical oxidation. Despite BDD electrodes have the advantages of high oxygen evolution potential and superior electrochemical stability[12], its high cost, complex preparation process and especially the difficulties to seek an appropriate substrate for deposition limit its application, only for the experimental study[10, 13]. Hence, the main problems hindering practical use are relatively high operating cost and short service life.

Due to its low cost, good conductivity, high oxygen over-potential and better electrochemical stability[14], the PbO_2 electrode has been widely used in electro-synthesis, electrolysis and more recently wastewater treatment process. In order to further improve the performance of PbO_2 electrode, a great deal of effort is being spent on some new methods, such as the adding of new intermediate layer (such as Sb-SnO_2[15], MnO_2[16], RuO_2[5]) between the titanium substrate and oxidation layer, doping metal or non-metallic ions

[a]College of Environmental Science and Engineering, Donghua University, Shanghai 201620, China. E-mail: chendhsit@163.com; Tel: +8613817007038.

[b]School of Chemical and Environmental Engineering, Shanghai Institute of Technology, Shanghai 201418, China

† Footnotes should appear here.

(such as Bi^{3+}, F^{-},Fe^{3+},Ce^{3+}) into the oxide layer[14], and using new preparation technologies[17]. However, the above methods still has inevitable limitations, and little effort has been spent on the research of improvement for titanium substrate.

Owing to its excellent physical and chemical properties (high tensile strength, low density and good chemical stability[9]), planar Ti has been widely accepted for substrates of electrodes coating, but the problem of poor adhesion of oxides active layer deposited on planar titanium would affect service life. Recently, as a novel titanium matrix, porous Ti has the advantages of good conductivity, corrosion resistance, high porosity, large surface area and good biocompatibility. It is widely used in aerospace, medical and chemical fields[18]. In addition, porous Ti substrates used as electrode substrate material also has attracted much more attention. Recent studies reveal the significance of porous Ti on improving the performance of electrodes. Braga et al. investigated that diamond grown on 3D porous titanium matrix with high roughness, large porosity and large surface area has outstanding electrochemical performance[19]. Sun.et at. studied that high quality BDD thin film electrodes deposited on porous Ti substrate were prepared successfully using the hot filament chemical vapour deposition (HFCVD) methods[20]. Zhang.et at. found that porous titanium substrate could effectively lower the charge transfer resistance in electro-deposition process and 3D-Ti/PbO_2 had abundant crystal orientations and large electrochemical active surface area[21, 22].

This work focuses on the investigation of the structure and electrochemical performance of porous Ti as PbO_2 electrode substrates. A systematic study was therefore carried out to investigate the preparation and characterization of porous Ti/SnO_2-Sb_2O_3/PbO_2 and planar Ti/SnO_2-Sb_2O_3/PbO_2. In addition, research shows that Ti-substrate PbO_2 anodes coated with a Sb-SnO_2 interlayer can increase service life and improve the performance of electro-catalytic oxidation[9]. Hence, SnO_2-Sb_2O_3 was chosen as intermediate layer by thermal decomposition and PbO_2 as oxides active layer by electrochemical deposition respectively. The morphology, crystalline structure, electrochemical performance, and stability of the prepared electrode were characterized. In order to further evaluate the electro-catalytic activity, methylene blue trihydrate was used as the model organic pollutant for electrochemical degradation. We hope that the experimental results can contribute to the development of porous titanium substrate as electrode materials.

2. Expermental

2.1 Materials and Reagents

Porous Titanium (purity 99.9%, 20 mm×10 mm×1 mm) and pure titanium sheets(TA2, 20 mm×10 mm×1 mm)were purchased from Baoji Jinkai Industrical Techanology Co.,Ltd. $SnCl_4$•$5H_2O$, $SbCl_3$,HCl, $Pb(NO_3)_2$, NaF and other chemicals used in this study were analytical grade and obtained from Sinopharm Chemical Reagent Co.,Ltd (Shanghai, China). All chemicals used in the experiment were received without further purification. All solution was prepared with deionized water

2.2 Electrode preparation

2.2.1 Titanium surface treatment

In order to prepare for a good adhesive metal oxide film material, both planar titanium and porous titanium substrate were pre-treated according to the same following procedures. Firstly, a porous titanium (20 mm×10 mm×1 mm) was mechanically polished with 600-grid abrasive papers. Then the porous titanium was cleansed with deionized water and acetone to remove solid particles and grease. Secondly, it was subsequently immersed in sodium hydroxide (15% m/m) at the temperature of 60 ℃ for 30 min and then was etched in boiling Hydrochloric acid (30% v/v) about 60 min to produce a gray surface with uniform roughness. Finally, it was washed by ultrasonic cleaning in ultrapure water and reserved in deionized water.

2.2.2 Coating SnO_2-Sb_2O_3

In the step, the SnO_2-Sb_2O_3 intermediate layer was prepared on titanium substrates by thermal decomposition described in reference[23]. The coating solution consisted of 6.65 g $SnCl_4$·$5H_2O$、0.475 g $SbCl_3$ and 1 mL concentrated HCl were dissolved in 25 ml isopropanol. The treated titanium substrate was dipped in the solution for 5 min, and then dried at about 130 ℃ for 10 min with excess solvent being evaporated by hot air, then the treated titanium substrate was calcined at 500 ℃ for 15 min in muffle furnace. All the above processes were repeated twelve times and the electrodes were annealed at 500 ℃ for 60 min in the last time. The purpose of the preparation of SnO_2-Sb_2O_3 intermediate layer is to increase the conductivity and prevent the formation of TiO_2 descried as in the related reference[15, 23].

2.2.3 Electrochemical deposition PbO_2

PbO_2 was deposited onto Ti/SnO_2-Sb_2O_3 (geometric area: 1.0×1.0 cm^2) under the current density of 20 $mA·cm^{-2}$ at 65℃ for 1 h with magnetic stirring. The coating solution consists of 0.1 M HNO_3 acidic media containing 0.5 mol L^{-1} $Pb(NO_3)_2$ and 0.04 mol L^{-1} NaF. After electro-deposition, the modified electrode was rinsed with deionized water. Ti/PbO_2 electrode without interlayer made in the same method was used as a reference, In the electro-deposition system the copper foil electrode (20 mm×20 mm) as cathode.

2.3 Performance analysis

2.3.1 Physicochemical characterization

The surface morphologies of electrodes were characterized by a HITACHI S-3400N scanning electron microscope. A PANalytical X'Pert PRO X-ray diffractometer with Cu Kα (λ=0.15418nm) incident radiation was employed to analysis the crystal structure of electrodes. The X-ray diffraction (XRD) patterns were taken for 2θ angles from 20° to 90° at a scan rate of 0.02° min^{-1}.

2.3.2 Electrochemical measurement

All electrochemical measurement of PbO_2 electrodes were tested on CHI760D electrochemical workstation (Chenhua Instrument Shanghai Co., Ltd, China) with conventional three-electrode cell. The three-electrode system was used with the PbO_2 electrodes as the working electrode, a saturated calomel electrode (SCE) as the reference electrode and a platinum sheet electrode as the counter electrode. Linear sweep voltammetry curves were performed to test

the oxygen evolution potential in 0.5 mol L^{-1} H_2SO_4 solution. Cycle voltammetry curves were recorded to calculate the votammetric charge quantity for different electrodes. The electrochemical impedance spectroscopy (EIS) was used to determine the charge transfer resistance of the modified electrodes. Anti-corrosion performance for electrodes was investigated using accelerate lifetime test with a current density of 500 mA cm^{-2} in 3.0 mol L^{-1} H_2SO_4 solution. The service life of the electrodes was considered to be terminated when the cell voltage reaches up to 10 V.

All electrochemical experiments were carried out at room temperature (25±2 ℃). All solutions were prepared with deionized water and all reagents used in the experiments were analytic grade.

2.4 Electro-catalytic test

Methylene blue trihydrate was used as the target pollutant for electrochemical degradation test. The electrochemical degradation was carried out in a cylindrical single compartment cell equipped with a magnetic stirrer and a jacketed cooler to maintain a constant temperature. The porous-PbO_2 electrode and planar-PbO_2 electrodes (1 cm × 1 cm) worked as the anode respectively. The cathode was stainless copper foil (2 cm × 2 cm), with a distance of 1.5 cm between the two electrodes. The initial methylene blue trihydrate was 10 mg L^{-1} and 0.1 mol L^{-1} Na_2SO_4 was added to the aqueous solution as the supporting electrolyte. The current density was controlled to be constant 60 mA cm^{-2} by a direct current power supply (RXN-605D, China). The stirring rate was about 800 r min^{-1}. The experiments were carried out at room temperature for 120 min. During the experiments, liquid samples were withdrawn from the electrolytic cell every 20 min for the TU-1810 UV/visible analysis Spectrophotometer (Beijing Puxi Instrument Co. Ltd.). The maximum adsorption wavelength of methylene blue trihydrate is 664 nm. The colour removal efficiency of methylene blue trihydrate in electrochemical oxidation can be calculated as follows:

$$\text{colour removal efficiency} = \frac{A_0 - A_t}{A_0} \times 100\%$$

Where A_0 is the absorbance value in 664 nm of initial wastewater sample and A_t is the absorbance value 664 nm of the wastewater samples at the given time t.

In addition, we used the fluorescence method based on terephthalic acid, a well know ·OH scavenger that can be used for estimation the amount of ·OH radicals generated under various conditions by a fluorescence spectrophotometer (Perkin Elmer LS-50, American). An aqueous solution of a volume of 200 mL containing 0.5 mol L^{-1} terephthalic acid, 0.5 g L^{-1} NaOH and 0.25 mol L^{-1} Na_2SO_4 was used as electrolytic solution. The anode was prepared PbO_2 electrode and the cathode was a stainless sheet. Hydroxyl radical production was performed at a current density of 30 mA cm^{-2} at 30℃. During the experiments, samples were drawn from the reactor every 5 min and diluted 10 times with deionized water, then analyzed by fluorescence spectrophotometer. The fluorescence spectra were recorded in the range of 380-520 nm, using an excitation wavelength at 315 nm.

3. Results and discussion

3.1 Surface morphology and crystal structure of electrode

3.1.1 Morphological analysis by SEM

The SEM cross-section morphology of two electrodes is shown in Fig.1. It can be clearly seen that planar Ti/SnO_2-Sb_2O_3 electrode has significant boundary between SnO_2-Sb_2O_3 intermediate layer and PbO_2 coating. The thickness of every layer was 293 μm, 99 μm respectively. For porous Ti/SnO_2-Sb_2O_3/PbO_2 electrode, SnO_2-Sb_2O_3 intermediate layer can't be easily distinguished, which was distributed on porous titanium substrate, including the surface, wall in pores, only PbO_2 coating layer with the thickness of 173 μm closely covering on the surface of the electrode.

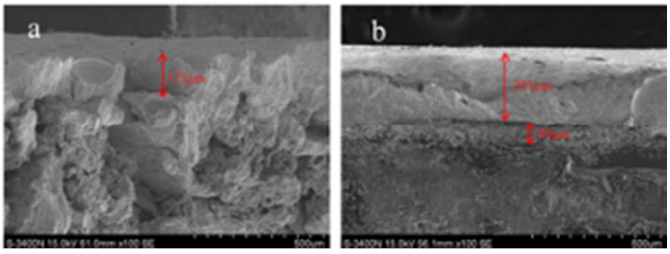

Fig.1 SEM morphology of Cross-sections for (a) porous Ti/SnO_2-Sb_2O_3/PbO_2 electrode(× 500), (b) planar Ti/SnO_2-Sb_2O_3 electrode.

Fig.2 shows the SEM surface micrographs of the prepared electrodes with different titanium substrate. All the insets correspond to the SEM with high magnification times. As can be seen from Fig.2(a) and Fig.2(b), Porous titanium substrate has different surface morphology and structure compared with the planar titanium substrate. It is clearly seen that the surface of the porous titanium was very rough and had irregular pores with average sizes of 30μm. The substrate can provide large specific surface area more than the planar titanium substrate.

Fig.2(c) and 2(d) show the morphological characteristics of the SnO_2-Sb_2O_3 intermediate layer deposited on the porous Ti and planar Ti substrate by thermal decomposition respectively. In comparison with Fig.2(c), the electrodes surface in Fig.2(d) exhibits a specific "crack-mud" micro-morphology structure which is typical for oxide electrodes as described by other literatures[9, 24]. On the contrary, the surface of the porous Ti/SnO_2-Sb_2O_3 electrode in Fig.2(c) appeared to be more compact, crack-free and uniformly distributed which is beneficial for electrochemical properties. The conclusion was further proved by the following experiments.

To further check the impact of porous Ti substrate on the formation of PbO_2, Fig.2(e) and 2(f) displays the electrode crystal structure and appearance of porous Ti/SnO_2-Sb_2O_3/PbO_2 and planar Ti/SnO_2-Sb_2O_3/PbO_2 with a magnification of 500 times, 4000 times of its insets. It is noticeable that particles sizes of porous Ti/SnO_2-Sb_2O_3/PbO_2 become smaller than that of planar Ti/SnO_2-Sb_2O_3/PbO_2 at the same magnification, the coating particles grown on the SnO_2-Sb_2O_3 intermediate layer did not present fissures or laminations and appeared to be more compact and uniformly distributed. The grain sizes of PbO_2 deposited on planar Ti/ SnO_2-Sb_2O_3 is almost ten times more than that of PbO_2 deposited on porous Ti/SnO_2-Sb_2O_3 which ranged from 200 nm to 450 nm, Similar results can be found in reference[21]. The porous Ti/SnO_2-

Sb_2O_3/PbO_2 electrode with nano-scale particles had larger specific surface area, which can provide more active sites for electrochemical oxidation. Hence porous Ti substrate-modified electrode was expected to have better electrochemical properties. This expectation has been proved by other authors[20].

In conclusion, despite using the same electrode preparation technology, porous titanium substrates resulted in an improved electrode with a different surface microstructure compared with the structure of electrode based planar titanium substrates. The underlying reason for the difference in the morphology of the two kinds of electrodes may be complicated. But porous titanium substrates with larger specific surface area and three-dimensional porous structure, is conducive to the uniform dispersion of the active coating with nano-structure. In addition, owing to the large surface area and more active sites, the porous Ti/SnO_2-Sb_2O_3 substrate could make the current distribution uniformly and reduce the current real density of electrode. Hence the potential of porous Ti/SnO_2-Sb_2O_3 is lower than that of planar Ti/SnO_2-Sb_2O_3 substrate. According to the crystal growth and nucleation theory, crystal growth is preferential at low potentials, and crystal nucleation is preferential at high potentials, the nucleation is preferential at high potentials on planar titanium substrates, large amounts of nuclei crash together to produce large particle as showed in Fig.2(f). While both the nucleation and growth are not preferential on the porous titanium substrates, many small crystallite particles have more chances to produce, leading to a uniform PbO_2 electrode.

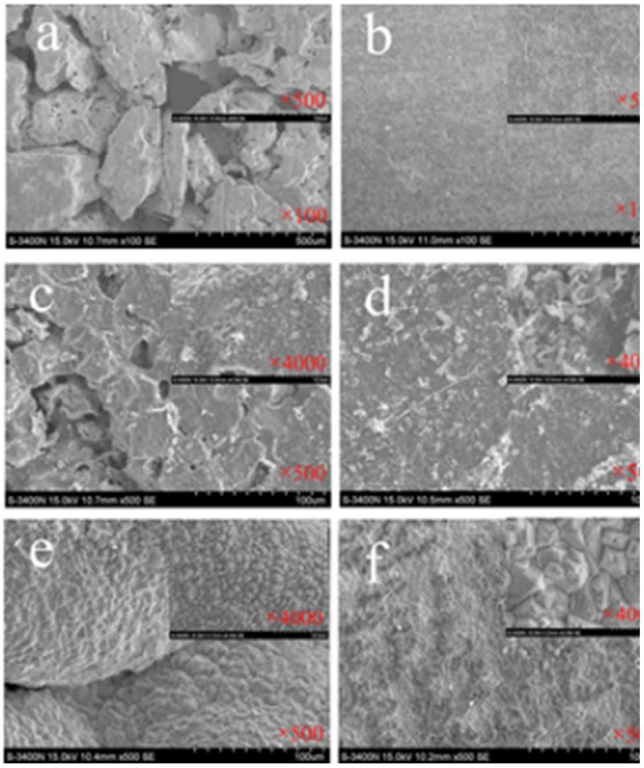

Fig.2 SEM images of (a) porous titanium substrate(× 500), (b) traditional planar titanium substrate(× 500), (c) porous Ti/SnO_2-Sb_2O_3 electrode(× 500), (d) planar Ti/SnO_2-Sb_2O_3 electrode(× 500), (e) porous Ti/SnO_2-Sb_2O_3/PbO_2 electrode(× 500), (f) planar Ti/SnO_2-Sb_2O_3/PbO_2 electrode(× 500); Inset: SEM images with high magnification (× 4000) corresponding to the electrode.

3.1.2.Structural analysis by XRD

In order to further verify the results of SEM observation and examine the crystalline structure and lattice parameters of the electrode coating, Fig.3A shows the wide-angle XRD analysis of different prepared electrodes based on planar and porous titanium substrates. A series of diffraction peaks of SnO_2, Sb_2O_3 and metal titanium structure were detectable for two samples in Fig.3A, and it is observed that the intensity of diffraction peaks for SnO_2 (110, 101, 211, 301) or Sb_2O_3 (022, 113, 361) of porous Ti/SnO_2-Sb_2O_3 electrode was much stronger than that of planar Ti/SnO_2-Sb_2O_3 electrode. No crystallized TiO_2 peaks were recorded, it strongly suggested that the Ti substrate was not oxidized in the process of thermal decomposition, and both porous and planar structure were not easy to completely be covered by the limited number of sintering. In order to fully cover the porous titanium matrix material, increasing the number of sintering could be beneficial.

It is well known that PbO_2 is polymorphic material with two allotropic forms, α-PbO_2 and β-PbO_2. The conductivity of β-PbO_2 is higher than that of α-PbO_2, indicating that the conductivity of PbO2 can be enhanced by increasing the β-PbO_2 content[25]. The corresponding patterns of the PbO_2 coatings with different substrate are shown in Fig.3B. It can be seen that the XRD of PbO_2 coatings based on different substrates are quite similar and the peaks intensity of PbO_2 deposited on porous Ti/SnO_2-Sb_2O_3 electrode are stronger than others of PbO_2. Among them, Fig.3(a) displays the main diffraction peaks at 2θ=25.4°, 32.0°, 36.2°, 49.2°, 52.1°, 59.2°, 62.3°, 74.4°, and 85.9° which are assigned to the (110), (101), (200), (211), (220), (310), (301), (321) and (411) planes of β-PbO2, and the strong main crystal plane of β-PbO2 is (101), (211) and (301) plane. At the same time, some weak peaks (2θ=67.8°, 76.9°) infer the presence of a-PbO_2. However, no diffraction peaks of tin and antimony oxides are observed, indicating that the active layer of PbO_2 was uniform and thus tin and antimony oxides were undetected by XRD. This was also confirmed by the above SEM results.

According to the electrochemical deposition mechanism of PbO_2 coatings as following[26]:

$$H_2O \rightarrow \cdot OH + H^+ + e \quad (1)$$

$$Pb^{2+} + \cdot OH \rightarrow Pb(OH)^{2+} \quad (2)$$

$$Pb(OH)^{2+} + H_2O \rightarrow Pb(OH)_2^{2+} + H^+ + e \quad (3)$$

$$Pb(OH)_2^{2+} \rightarrow PbO_2 + 2H^+ \quad (4)$$

In the process of electro-deposition, the ·OH group generated from equation (1) would adsorb on the PbO_2 crystal face and make crystal grow via equation (2) to (4). In addition, under the same conditions, the morphological difference of crystal produced should be attributed to the surface morphology and structure of substrates. Hence, the surface properties of porous Ti/SnO_2-Sb_2O_3 electrodes determine the nucleation free energy, and subsequently the nucleation and growth process also determines the crystal size, number and morphology of PbO_2 coating. The surface energy of the porous electrode with porous structure and roughness is greater than that of other planar electrode, which is helpful to overcome

interfacial energy and reduces the net interface energy of nucleation of. Therefore, it is advantageous to adsorb Pb^{2+} and ·OH on the electrode surface to form large number of crystal nuclei, but because of the limited total amount of ions in solution under the certain current density, the growth of PbO_2 crystal grains is limited. Thus, the limitation of the growth of PbO_2 crystal grains increases the chance of crystal nucleus growth. This led to a uniform and smooth PbO_2 electrode surface[27].

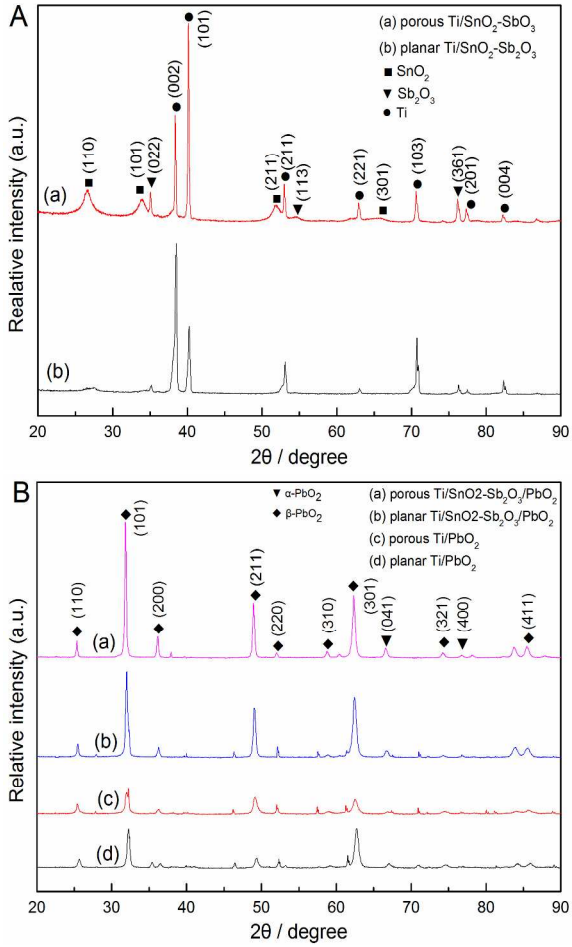

Fig.3 (A) XRD patterns of (a) porous Ti/SnO_2-Sb_2O_3 electrode, (b) planar Ti/SnO_2-Sb_2O_3 electrode. (B) XRD patterns of (a) porous Ti/SnO_2-Sb_2O_3/PbO_2 electrode, (b) planar Ti/SnO_2-Sb_2O_3/PbO_2 electrode, (c) porous Ti/PbO_2 electrode, (d) planar Ti/PbO_2 electrode.

3.2 Electrochemical characterization of electrode

3.2.1 Linear polarization curves

The oxygen evolution reaction (OER) is taken place when the current densities abruptly increase in the linear polarization curve. The over-potential for OER is obtained by an extrapolated technique from the polarization curve[10, 28-31]. Fig.4 displays the linear polarization curves of different electrodes in 0.5 mol L^{-1} H_2SO_4 solution at the scan rate of 20 mV s^{-1}. It shows that porous Ti/SnO_2-Sb_2O_3/PbO_2 had a higher oxygen evolution potential of 1.8V which is higher than that of planar Ti/SnO_2-Sb_2O_3/PbO_2, porous Ti/PbO_2 and planar Ti/PbO_2 in this comparison experiment and other PbO_2 or Ti-based modified electrodes, such as 1.75V for Ti/PbO2-Sn[29], 1.61V for CNT-Bi-PbO_2[32] and 1.6V for β-PbO_2[33]. Tafel plots is another method to evaluate the oxygen evolution reaction[34, 35]. We adopt the method to further support the above results. From the inset of Fig.4, it can be seen that the porous Ti/SnO_2-Sb_2O_3/PbO_2 electrode was characterized by high oxygen evolution over-potential (OEP) and follow the Tafel relation, with a slope at 170 mV $decade^{-1}$. For the planar Ti/SnO_2-Sb_2O_3/PbO_2 electrode, a lower Tafel slope, 140 mV $decade^{-1}$ is found. The results indicate the OEP of porous Ti/SnO_2-Sb_2O_3/PbO_2 electrode is higher than that of planar Ti/SnO_2-Sb_2O_3/PbO_2 electrode which was in accord with the results of an extrapolated technique from the polarization curve. Obviously, adopting porous titanium can significantly enhance the oxygen evolution over-potential of PbO_2 electrode. In general, high oxygen evolution over-potential would restrain the evolution of oxygen molecule which would be beneficial for the efficiency of organic pollutant degradation during the electro-catalytic oxidation process.

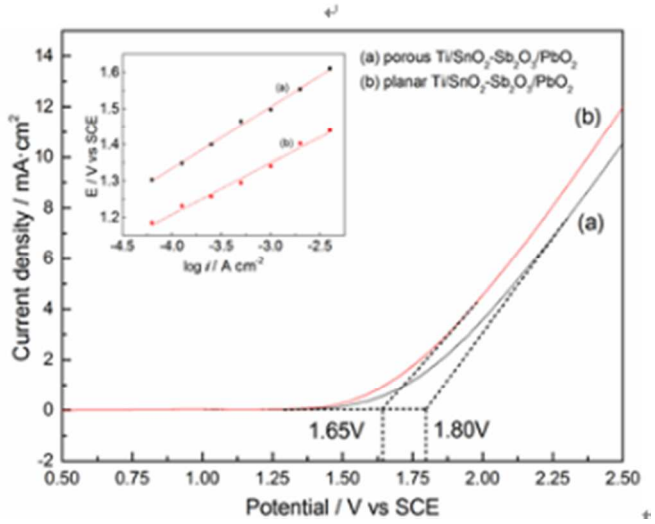

Fig.4 Linear polarization curves of different PbO_2 electrodes in 0.5 mol L^{-1} H_2SO_4 solution, scan rate: 20 mV S^{-1}, inset of Tafel plots for oxygen evolution reaction.

3.2.2 Electrochemical active surface area

Electrochemical active surface area means that the active sites are accessible to electrolyte when electrochemical reaction occurs[36]. It is known that the real surface area of electrode especially for porous electrodes, was related to the voltammetric charge (q^*)[37-39]. Hence, we used the method reported by other references [36, 40] to quantify the electrode areas. The total electrochemical surface area (q_T^*) was calibrated through ploting the reciprocal of q^* against the square root of the potential scan rate by using the following equation:

$$(q^*)^{-1} = (q_T^*)^{-1} + kv^{1/2} \quad (5)$$

The q_T^* is composed of two fractions, q_0^* and q_i^*, which represent electric quantity in the outer geometric and inner unattainable electrode areas respectively. The values of outer charge q_0^* and q_i^* can be obtained according to the equation:

$$q^* = q_0^* + kv^{-1/2} \quad (6)$$

$$q_T^* = q_0^* + q_i^* \quad (7)$$

The values of the inner charge (q_i^*) can be acquired by the subtraction of q_T^* and q_0^*. The electrochemical porosity is defined as the ration between the inner and total charge (q_i^*/ q_T^*). v stands for the scan rate of voltage, while k is a constant.

The relationship of the reciprocal of q^* versus square root of scan rate is shown in Fig.5A and satisfactory linear fitting are obtained. Through extrapolating the linear plots v = 0, the total electrochemical surface area q_T^* was obtained. In addition, the values of outer charge q_0^* could be obtained from the extrapolating of $v \approx \infty$ according to equation (6) in Fig.5B. The values of the charges and electrochemical porosity for the different electrodes were list in Table 1.

The results indicated the adopting porous titanium substrate could cause an increase of the effective surface area and voltammetric charge. The inner quantity q_i^* of porous Ti/PbO_2 is approximately 100 times that of planar Ti/PbO_2. At the same time, PbO_2 deposited on porous titanium substrate had higher electrochemical porosity which was in accordance with SEM analysis of Fig.1 and Fig.2. Hence, porous titanium could provide with more real surface areas to active sites for electro-catalytic oxidation.

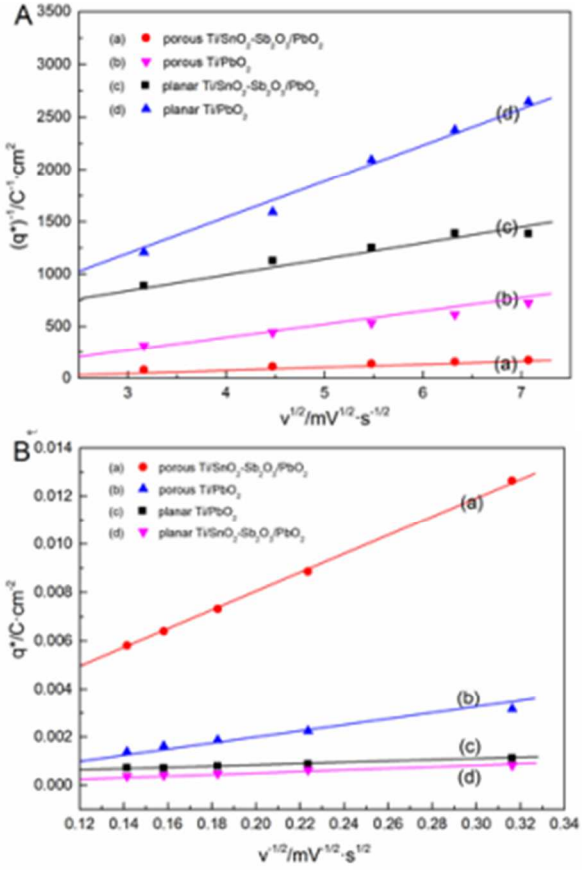

Fig.5 (A) Extrapolation of q_T^* for electrodes from the representation of $(q^*)^{-1}$ versus $v^{1/2}$, (B) Extrapolation of q_0^* for electrodes from the representation of q^* versus $v^{-1/2}$: data obtained the cyclic voltammograms obtained between 0.3 and 0.8V versus SCE in 0.5 mol.L^{-1} H_2SO_4 solution at scan rate of from 10 to 50 mV s^{-1}.

Table 1 The data of total, outer and inner charges, electrochemical porosity obtained for voltammetric charge analyses of various electrode.

Electrode	q_T^* ($C \cdot cm^{-2}$)	q_0^* ($C \cdot cm^{-2}$)	q_i^* ($C \cdot cm^{-2}$)	q_i^*/q_T(%)
planar Ti/PbO_2	0.000927	0.0005	0.000427	46.06
planar Ti/SnO_2-Sb_2O_3/PbO_2	0.001979	0.0004	0.001579	79.79
porous Ti/PbO_2	0.044395	0.0014	0.042995	96.84
porous Ti/SnO_2-Sb_2O_3/PbO_2	0.188360	0.0050	0.183360	97.34

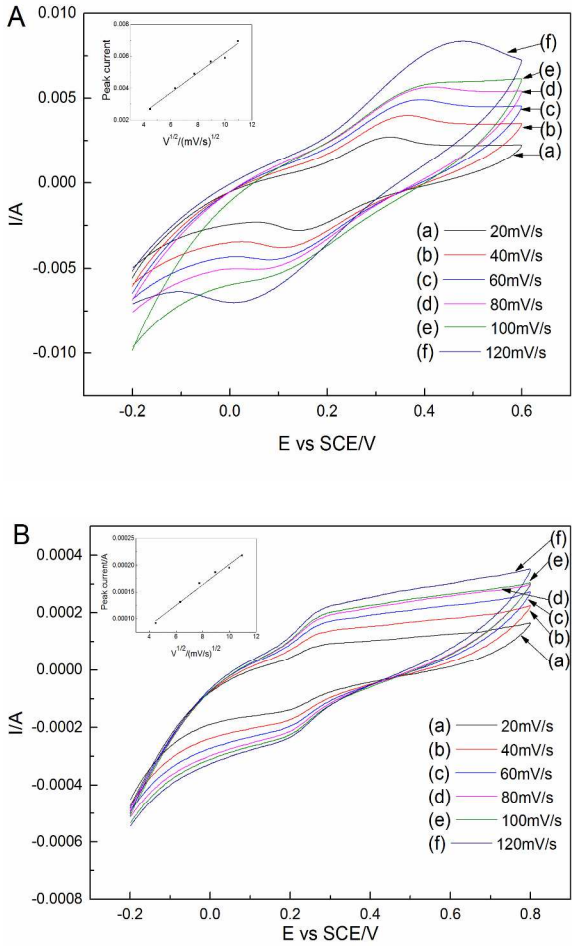

Fig.6 Cyclic votammograms of different PbO_2 electrodes in 50 mmol L^{-1} $K_3Fe(CN)_6$ +1 mol L^{-1} KCl solution with different scan rate. (A) porous Ti/SnO_2-Sb_2O_3/PbO_2 electrode, (B) planar Ti/SnO_2-Sb_2O_3/PbO_2. Insets show the plots of peak current vs. the square root of scan rate.

3.2.4 Electrochemical impedance

Fig.7 displays electrochemical impedance of planar Ti/SnO_2-Sb_2O_3/PbO_2 (a) and porous Ti/SnO_2-Sb_2O_3/PbO_2 electrode (b) in 0.5 mol L^-

[1] H_2SO_4 solution at oxygen evolution region (1.85 V vs SCE). The equivalent circuit shown in Figure.8 was used to fit the EIS data. The simulated data of each parameter in Fig.8 is listed in Table 2. In this $R_s(R_{ct}Q_{dl})$ circuit, R_s represents ohmic resistance including the resistance of electrolyte and active material. R_{ct} stands for charge-transfer resistance, reflecting oxygen evolution reaction activity. Q_{dl} is introdued to replace the electric double layer capacitor.

It can be seen clearly from Fig.7 that two obvious semicircles appeared in electrochemical impedance spectra. The diameter of the semicircle size reflects R_{ct} and the resistance values were 1.742 Ω•cm^2 and 0.715 Ω•cm^2 in Table 2 respectively, indicating that the oxygen evolution reaction activity of porous Ti/SnO_2-Sb_2O_5/PbO_2 electrode was higher. According to the reaction mechanism of electrode oxygen evolution[16, 41], the oxygen evolution activity depends on the active sites of active coating, the more the active sites, the greater the reaction activity. Hence the porous Ti/SnO_2-Sb_2O_5/PbO_2 electrode with larger specific surface area has much more activity, resulting in oxygen evolution activity. The result was further proved by the R_s values in Table 2 that the porous Ti/SnO_2-Sb_2O_3/PbO_2 electrode prepared had the smallest R_s, indicating the largest electrochemical active surface area. From the above results, it can conclude that porous titanium substrates can reduce the R_s and R_{ct}, meaning the conductivity and electrochemical activity of oxygen evolution are higher than those for the planar titanium substrates electrode. In addition, high electrochemical active surface is important to prepare high performance electrode.

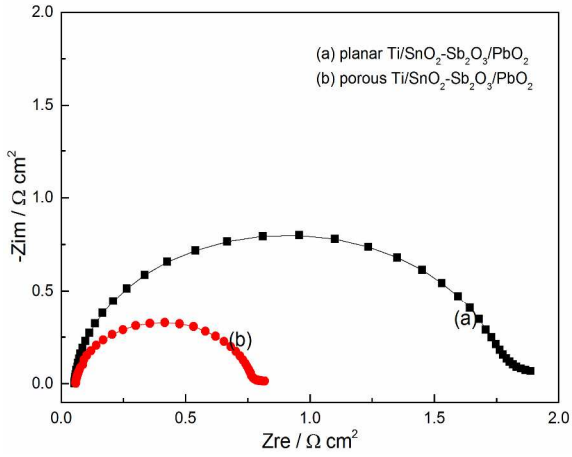

Fig.7 EIS plots in the 0.5 mol L^{-1} acidic solution: (a) planar Ti/SnO_2-Sb_2O_3/PbO_2, (b)porous Ti/SnO_2-Sb_2O_3/PbO_2 electrode. Electrode potential: 1.85 V vs SCE.

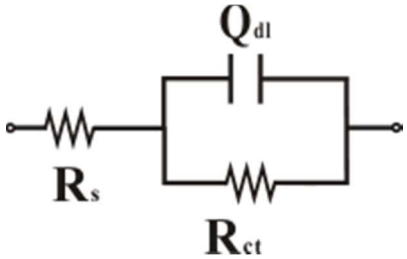

Fig.8 Equivalent circuit used in the analysis of the experimental EIS data.

Table 2 Simulated values of each electrical element

Electrode	R_s/Ω cm^2	Q_{dl}/Ω cm^{-2}s^n	R_{ct}Ω/Ω cm^2	n
planar Ti/SnO_2-Sb_2O_3/PbO_2	0.5889	0.0018	1.742	0.9653
porous Ti/SnO_2-Sb_2O_3/PbO_2	0.3412	0.0056	0.715	0.9591

3.2.5 Electrode stability

As shown in Fig.9, porous Ti/SnO_2-Sb_2O_3/PbO_2 exhibited the best electrochemical stability and its service lifetime was the longest (214 h), as much as 3.69 times that of planar Ti/SnO_2-Sb_2O_3/PbO_2 (58 h), then porous Ti/PbO_2 electrode (0.5 h) and last planar Ti/PbO_2 electrode (2.3 h). The results reveal that porous titanium as the substrate materials for prepared electrode can improve the electrochemical stability of PbO_2 electrode. It can be explained by the following reasons.

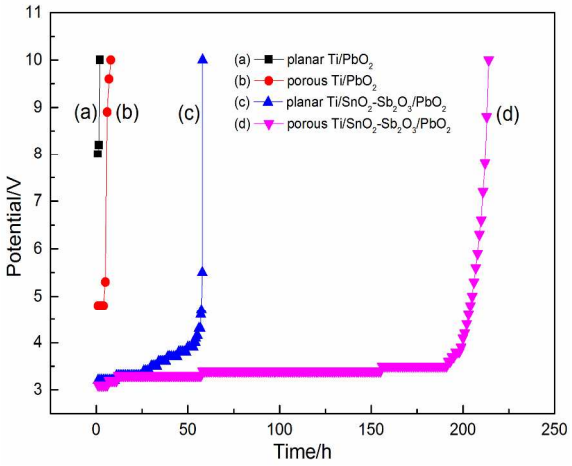

Fig.9 Variation of cell potential with the testing time in the accelerated life for different PbO_2 electrodes.

Firstly, it resulted from the decrease of the PbO_2 particle size which can make a compact and fine surface layer as observed from the SEM images in Fig.2. The compact surface of porous Ti/SnO_2-Sb_2O_3/PbO_2 can baffle the penetration of the supporting electrolyte toward the titanium substrate through the cracks and pores and delay the formation of non-conductive TiO_2 layer. Additionally, The surface properties of porous titanium itself can make SnO_2-Sb_2O_3 interlayer or PbO_2 film and substrate combine more tightly and reduced the film detachment[22]. Secondly, the oxygen evolution over-potential of electrode has an important impact on the electrochemical stability. The evolution of oxygen on the anode will result in the stripping and dissolution of PbO_2 film. Hence, when the oxygen evolution over-potential increased, the process of evolution of oxygen reduced, which could prolong the lifetime of electrode. Thirdly, compared with Ti/PbO_2 electrode without SnO_2-Sb_2O_3 interlayer, porous Ti/SnO_2-Sb_2O_3/PbO_2 or planar Ti/SnO_2-Sb_2O_3/PbO_2 showed better electrochemical stability. The reason is that Sb-doped SnO_2 interlayer can further reduce the internal stress with titanium substrate and improve the stability[42].

3.3 Electro-catalytic test

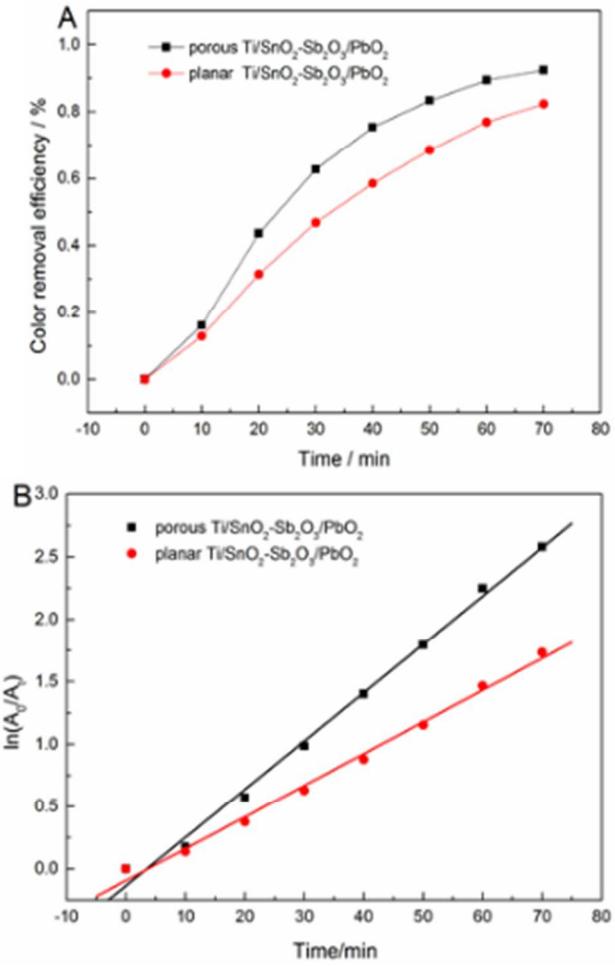

Fig.10 Colour removal efficiency as a function of degradation time for different electrodes during electrolysis of methylene blue trihydrate: (A). Operating condition: Na_2SO_4 concentration, 0.1 mol L^{-1}; initial concentration, 10 mg L^{-1}; Current density: 60 mA cm^{-2} ; stirring rate: 800 r min^{-1} (B). Kinetic analysis of the curves.

To investigate the influence of porous titanium substrate on the electro-catalytic degradation activity of the prepared electrode, degradation experiments were carried on different electrode. The variations of colour removal efficiency for methylene blue trihydrate with electrolysis time are shown in Fig.10A. It can be clearly seen that the colour removal efficiency rates are up to 90% within 70min for porous Ti/SnO_2-Sb_2O_3/PbO_2 electrode, only 76% for planar Ti/SnO_2-Sb_2O_3/PbO_2 electrode. Porous titanium electrodes showed the highest activity for colour removal. In addition, the degradation processes were fitted by pseudo-first-order model for all electrodes. And the fitting results were shown in Fig.10B. According to the good linear correlation between the logarithm values of the normalized concentration and de-colorization time, the degradation of methylene blue trihydrate on these electrodes fitted to the pseudo-first-order kinetics, and the rate equation for the de-colorization can be expressed as follows:

$$C_t = C_0 e^{-k_{app}t} \qquad (9)$$

Where k_{app} is the apparent kinetics coefficient. The k_{app} values for the two electrodes were 0.03868 min^{-1} and 0.02542 min^{-1} respectively.

It is clearly from Fig.10 and kinetics coefficient k_{app} value that porous titanium electrodes displayed better de-colorization performance for degradation of methylene blue trihydrate. The reaction rate constant of porous titanium electrodes was 1.52 times than that of planar titanium electrodes. The highest de-colorization rate can be ascribed to the highest active surface area for porous electrodes which can provide more active site to generate more ·OH radicals. At the same time, a large surface area increased the adsorption ability of reagent and ·OH radicals, which resulted in an improvement of de-colorization ability.

It is well known that pollutants are mainly degraded by the indirect electrochemical oxidation mediated by ·OH radicals in the electro-catalytic oxidation process. Hence, the ·OH radicals generation ability can give more accurate information about electro-catalytic ability of electrode materials. During electrochemical treatment, terephthalic acid as a kind of ·OH radicals capture agent, can readily react with ·OH radicals to produce highly fluorescent product 2-hydroxyterephthalic acid. The amount of ·OH radicals formed was approximately equal to the amount of 2-hydroxyterephthalic acid, which was represented with the intensity of fluorescence intensity[43]. As can be seen in Fig.11, the fluorescence intensity of 2-hydroxyterephthalic acid around 425 nm for two electrodes increased with increasing the reaction time, indicating that ·OH radicals were indeed formed on the anodes and played an important role in electrochemical degradation test. Comparing the fluorescence intensity for different electrodes at different reaction time, it is found that the fluorescence intensity for porous Ti/SnO_2-Sb_2O_3/PbO_2 electrode was higher than that for planar Ti/SnO_2-Sb_2O_3/PbO_2 electrode, which revealed the excellent electro-catalytic activity of porous PbO_2 electrode. Therefore, porous Ti/SnO_2-Sb_2O_3/PbO_2 electrode could oxidize pollutants more effectively compared with planar electrode.

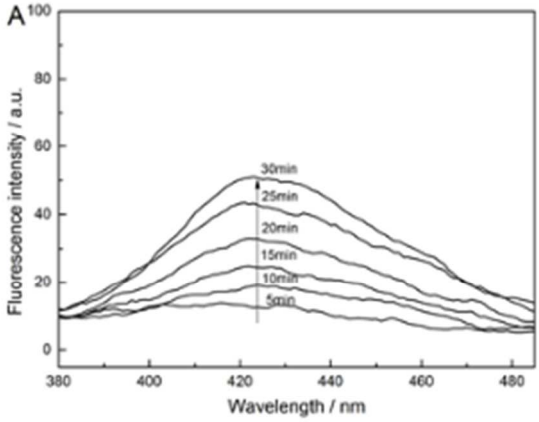

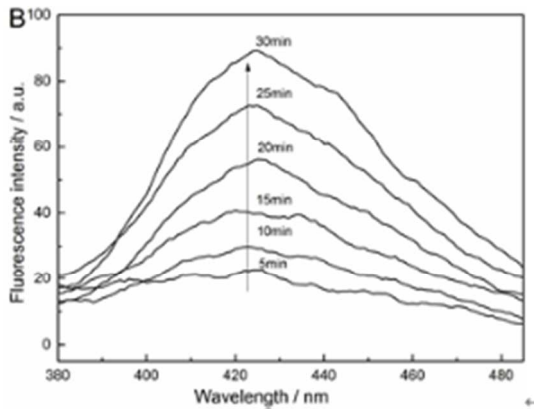

Fig.11 Fluorescence spectra changes observed during electro-catalytic oxidation process in 0.5 mol L^{-1} aqueous solution of terephthalic acid using prepared PbO_2:(A)planar Ti/SnO_2-Sb_2O_3/PbO_2 , (B) porous Ti/SnO_2-Sb_2O_3/PbO_2 electrode.

4. Conclusions

The porous Ti/SnO_2-Sb_2O_3/PbO_2 electrode was successfully prepared on a porous titanium substrate by thermal decomposition and electro-deposition method respectively. The surface morphology and structure of porous Ti/SnO_2-Sb_2O_3 or porous Ti/SnO_2-Sb_2O_3/PbO_2 electrode showed that porous structure could be beneficial for physicochemical characterization of electrodes. The surface structure of porous Ti substrate and porous Ti/SnO_2-Sb_2O_3 can improve interlayer coating structure effectively and favors the formation of PbO_2 during electrodeposition. The linear polarization curves show that the overpotential for OER of PbO_2 electrode based on porous titanium substrates is higher when compared to planar titanium substrate electrode. The voltammetric charge quantity indicated that the porous Ti/SnO_2-Sb_2O_3/PbO_2 electrode had the highest active surface area. The cyclic voltammetry analysis demonstrated that the porous Ti substrate enhanced the mass transfer rate on PbO_2 electrode. The results of accelerated life tests showed that the service life of porous Ti/SnO_2-Sb_2O_3/PbO_2 electrode was longer than those of three other kinds of electrodes, which was 3.69 times that of planar Ti/SnO_2-Sb_2O_3/PbO_2. Due to its highest over-potential and large active surface area, the porous Ti/SnO_2-Sb_2O_3/PbO_2 electrode showed the best degradation performance in the simulated wastewater treatment. Its pseudo first-order kinetics coefficient is 0.03868min^{-1}. In summary, porous titanium substrates are importance for the performance improvement of electrodes.

Acknowledgements

The authors are grateful for the financial support provided by the Innovative Program of Activities for University in Shanghai (NO. PE2015029). Wenli Zhang (Jilin University) and Quansheng Zhang (Shanghai Institute of Technology) are also gratefully acknowledged for supplying experimental guidance and the electrochemical workstation, respectively.

References

1. M. Zhou, Q. Dai, L. Lei, C. a. Ma and D. Wang, *Environmental science & technology*, 2004, **39**, 363-370.
2. C. Comninellis, *Electrochimica Acta*, 1994, **39**, 1857-1862.
3. M. Panizza and G. Cerisola, *Chemical Reviews*, 2009, **109**, 6541-6569.
4. C. A. Martinez-Huitle and S. Ferro, *Chemical Society Reviews*, 2006, **35**, 1324-1340.
5. N. Fan, Z. Li, L. Zhao, N. Wu and T. Zhou, *Chemical Engineering Journal*, 2013, **214**, 83-90.
6. W. Wu, Z.-H. Huang and T.-T. Lim, *Applied Catalysis A: General*, 2014, **480**, 58-78.
7. X.-y. Li, Y.-h. Cui, Y.-j. Feng, Z.-m. Xie and J.-D. Gu, *Water research*, 2005, **39**, 1972-1981.
8. M. M. Dong, R. Trenholm and F. L. Rosario-Ortiz, *Journal of hazardous materials*, 2014.
9. D. Shao, X. Li, H. Xu and W. Yan, *RSC Advances*, 2014, **4**, 21230-21237.
10. G. Zhao, Y. Zhang, Y. lei, B. Lv, J. Gao, Y. Zhang and D. Li, *Environmental science & technology*, 2010, **44**, 1754-1759.
11. S. Chen, Y. Zheng, S. Wang and X. Chen, *Chemical Engineering Journal*, 2011, **172**, 47-51.
12. M. Panizza and G. Cerisola, *Electrochimica Acta*, 2005, **51**, 191-199.
13. G. Zhao, P. Li, F. Nong, M. Li, J. Gao and D. Li, *The Journal of Physical Chemistry C*, 2010, **114**, 5906-5913.
14. W. Wu, Z.-H. Huang and T.-T. Lim, *Applied Catalysis A: General*, 2014, **480**, 58-78.
15. H.-y. Ding, Y.-j. Feng and J.-f. Liu, *Materials Letters*, 2007, **61**, 4920-4923.
16. Z.-G. Ye, H.-M. Meng and D.-B. Sun, *Journal of Electroanalytical Chemistry*, 2008, **621**, 49-54.
17. Q. Wang, T. Jin, Z. Hu, L. Zhou and M. Zhou, *Separation and Purification Technology*, 2013, **102**, 180-186.
18. M. Manjaiah, S. Narendranath and S. Basavarajappa, *Transactions of Nonferrous Metals Society of China*, 2014, **24**, 12-21.
19. N. A. Braga, C. A. A. Cairo, E. C. Almeida, M. R. Baldan and N. G. Ferreiraa, *Diamond and Related Materials*, 2008, **17**, 1891-1896.
20. J. Sun, H. Lu, H. Lin, W. Huang, H. Li, J. Lu and T. Cui, *Materials Letters*, 2012, **83**, 112-114.
21. W. Zhang, H. Lin, H. Kong, H. Lu, Z. Yang and T. Liu, *Electrochimica Acta*, 2014, **139**, 209-216.
22. W. Zhang, H. Lin, H. Kong, H. Lu, Z. Yang and T. Liu, *International Journal of Hydrogen Energy*, 2014, **39**, 17153-17161.
23. H. An, Q. Li, D. Tao, H. Cui, X. Xu, L. Ding, L. Sun and J. Zhai, *Applied Surface Science*, 2011, **258**, 218-224.
24. F. Montilla, E. Morallón, A. De Battisti and J. Vazquez, *The Journal of Physical Chemistry B*, 2004, **108**, 5036-5043.
25. X. Yang, R. Zou, F. Huo, D. Cai and D. Xiao, *Journal of hazardous materials*, 2009, **164**, 367-373.
26. X. Hao, S. Dan, Z. Qian, Y. Honghui and W. Yan, *RSC Advances*, 2014, **4**, 25011-25017.
27. R. XIUBIN, L. HAIYAN, L. YANAN, L. WEI and L. HAIBO, *3-Dimensional Growth Mechanism of Lead Dioxide Electrode on the Ti Substrate in the Process of Electrochemical Deposition*, Kexue Chubanshe, Beijing, CHINE, 2009.
28. Y. Liu, H. Liu, J. Ma and J. Li, *Electrochimica Acta*, 2011, **56**, 1352-1360.
29. H. Li, Y. Chen, Y. Zhang, W. Han, X. Sun, J. Li and L. Wang, *Journal of Electroanalytical Chemistry*, 2013, **689**, 193-200.
30. L. Zhang, L. Xu, J. He and J. Zhang, *Electrochimica Acta*, 2014, **117**, 192-201.
31. M. Panizza, P. A. Michaud, G. Cerisola and C. Comninellis, *Electrochemistry Communications*, 2001, **3**, 336-339.
32. L. Chang, Y. Zhou, X. Duan, W. Liu and D. Xu, *Journal of the Taiwan Institute of Chemical Engineers*, 2014, **45**, 1338-1346.
33. Y. J. Feng and X. Y. Li, *Water research*, 2003, **37**, 2399-2407.

34. B. Correa-Lozano, C. Comninellis and A. D. Battisti, *Journal of Applied Electrochemistry*, 1997, **27**, 970-974.
35. Y. Dan, H. Lu, X. Liu, H. Lin and J. Zhao, *International Journal of Hydrogen Energy*, 2011, **36**, 1949-1954.
36. H. Vogt, *Electrochimica acta*, 1994, **39**, 1981-1983.
37. Y. Takasu and Y. Murakami, *Electrochimica acta*, 2000, **45**, 4135-4141.
38. S. Ardizzone, G. Fregonara and S. Trasatti, *Electrochimica Acta*, 1990, **35**, 263-267.
39. F. Montilla, E. Morallón, A. De Battisti and J. L. Vázquez, *The Journal of Physical Chemistry B*, 2004, **108**, 5036-5043.
40. Y. Chen, L. Hong, H. Xue, W. Han, L. Wang, X. Sun and J. Li, *Journal of Electroanalytical Chemistry*, 2010, **648**, 119-127.
41. Z.-G. Ye, H.-M. Meng, D. Chen, H.-Y. Yu, Z.-S. Huan, X.-D. Wang and D.-B. Sun, *Solid State Sciences*, 2008, **10**, 346-354.
42. S. Chai, G. Zhao, Y. Wang, Y.-n. Zhang, Y. Wang, Y. Jin and X. Huang, *Applied Catalysis B: Environmental*, 2014, **147**, 275-286.
43. K.-i. Ishibashi, A. Fujishima, T. Watanabe and K. Hashimoto, *Electrochemistry Communications*, 2000, **2**, 207-210.

